

# A SIMPLE AND EFFICIENT FINITE ELEMENT FOR PLATE BENDING

THOMAS J. R. HUGHES\*

*Division of Engineering and Applied Science, California Institute of Technology, Pasadena, California, U.S.A.*

ROBERT L. TAYLOR† AND WORSAK KANOKNUKULCHAI‡

*Division of Structural Engineering and Structural Mechanics, Department of Civil Engineering, University of California, Berkeley, California, U.S.A.*

## SUMMARY

A simple and efficient finite element is introduced for plate bending applications. Bilinear displacement and rotation functions are employed in conjunction with selective reduced integration. Numerical examples indicate that, despite its simplicity, the element is surprisingly accurate.

## INTRODUCTION

An enormous amount of effort has been devoted to the development of finite elements for the bending of plates. The literature is extensive and we will not make an attempt to review it here. (The interested reader may consult any of the standard texts for references.<sup>1-3</sup>) Most of this effort has been oriented towards linear problems; in particular, to the classical Poisson-Kirchhoff theory of bending. The  $C^1$ -continuity requirement imposed by this theory on 'displacement' finite element models precludes the development of simple and natural elements.<sup>4</sup> Because of this, incompatible elements<sup>5,6</sup> are often resorted to, since they involve simpler programming than the rather complicated  $C^1$ -continuous elements<sup>6-8</sup> and are competitive from an accuracy standpoint.

Accurate higher-order  $C^1$ -elements have also been developed,<sup>9-11</sup> but they too are quite complicated and involve nodal derivative degrees-of-freedom of order greater than one, which complicates the specification of boundary conditions.

The assumed stress hybrid bending elements of Pian and his associates have often proved to be accurate, but they have some drawbacks and thus are not widely used.

Another approach to the development of bending elements for thin plates involves the so-called 'discrete Kirchhoff hypothesis'.<sup>13-14</sup> In this approach the classical equations are abandoned in favour of a bending theory which includes shear deformations. The result is that only  $C^0$ -continuity is required of the shape functions. To capture the behaviour of thin plate theory, the constraint of zero shear strains is imposed at a discrete number of points. The method is effective, but implementations tend to be somewhat complicated. Recent improvements and variants on this theme have been proposed by Fried.<sup>15-17</sup>

---

\* Assistant Professor of Structural Mechanics.

† Professor of Civil Engineering.

‡ Graduate Student.

*Received May 1976  
Revised 12 October 1976*

An accurate quadrilateral element for thick and thin plates has been developed by Zienkiewicz *et al.*<sup>18</sup> This element possesses eight nodes—four corner and four midside—with the basic three degrees-of-freedom per node. The transverse displacement and rotation shape functions are selected from the ‘serendipity’ family.<sup>1</sup> Two-by-two Gaussian quadrature is an essential requirement for the good performance of the element.

In summarizing these developments one can confidently assert that for linear problems of plate bending many adequate elements exist. The choice is more a matter of taste as no single element is clearly superior to the rest in all cases.

Many users of finite element computer programs find a ‘basic’ four-node quadrilateral element particularly appealing due to its simplicity. It is our feeling that this appeal will become even greater when non-linear applications are undertaken. In the non-linear regime—and especially in non-linear dynamics—computational cost is the prime concern. Due to frequent reformulations of tangent stiffnesses, complicated element routines can lead to exorbitant computational expenditures and may actually preclude non-linear analysis. A simpler element of competitive accuracy becomes quite desirable under such circumstances. Other factors in non-linear analysis support this viewpoint. For example the accuracy level attainable in non-linear problems is often severely limited due to the uncertainty of non-linear material characterizations. Thus it makes little sense to engender significant computational cost for complicated bending elements which are only marginally more accurate than simpler elements, since the confidence level of the overall analysis may be affected only negligibly. Unfortunately, heretofore, no really simple alternative has existed.

In this paper we attempt to remedy this situation. We develop what we believe is the *simplest effective plate bending element yet proposed*. The element is a four-node quadrilateral with the basic three degrees-of-freedom per node. The element shape functions are bilinear for transverse displacement and rotations. The shear ‘locking’ associated with such low-order functions in application to thin plates is alleviated by splitting the shear and bending energies and using one-point quadrature on the shear term. The simplicity of the element lends itself to concise and efficient computer implementation.

To develop the theory in its simplest setting, we consider in Section 2 ‘Example: linear beam element’ a beam element involving linear displacement and rotation shape functions. We show how exact integration (two-point Gaussian quadrature) of the element stiffness matrix leads to an overly stiff element and we present an heuristic argument why this is the case. We then show how employing one-point quadrature on the shear term lessens the stiffness. The concept is identical for the plate bending element which is developed in Section 3 ‘Bilinear plate bending element’. The effectiveness of the element in thin plate bending is demonstrated in Section 4 ‘Numerical examples: thin plates’. A simple computing strategy for dealing with the numerically sensitive case of extremely thin plates is presented in Section 5 ‘Numerical sensitivity due to extreme thinness’. Following this we consider applications to thick plates. It is shown that the element is still effective for moderately thick plates. However, for very thick plates, in which the thicknesses of individual elements exceed their characteristic lengths, a slight modification of the shear quadrature need be employed.

## EXAMPLE: LINEAR BEAM ELEMENT

In this section we will describe the formulation of a beam element stiffness for which displacement and rotation are assumed to be independent linear functions. Exact integration of the element stiffness can be facilitated by two-point Gaussian quadrature, whereas one-point integration exactly integrates the bending contribution, but ‘underintegrates’ the shear con-

tribution. For the case of thin beams we view the shear term as a constraint which attempts to enforce the condition of negligible shear strains. We shall show that one-point quadrature has a decisively positive effect on the accuracy of the element; two-point quadrature leading to worthless numerical results. *The upshot of all this is that by appropriately underintegrating troublesome terms, good bending behaviour can be attained by the simplest shape functions.*

The equations of a rectangular cross-section beam, including shear deformation effects, emanate from the following expression for strain energy:

$$U(w, \theta) = \frac{1}{2} \frac{Et^3}{12} \left[ \int_0^L \left( \frac{dw}{dx} \right)^2 dx + \kappa \frac{12G}{Et^2} \int_0^L \left( \frac{dw}{dx} - \theta \right)^2 dx \right], \quad (1)$$

where  $w$  is the transverse displacement of the centre-line,  $\theta$  is the rotation of the cross-section,  $E$  is Young's modulus,  $G$  is the shear modulus,  $\kappa$  is the shear correction factor (throughout we employ  $\kappa = 5/6$ ),  $t$  is the depth,  $L$  is the length and  $x$  is the axial co-ordinate. The first term on the right-hand side of (1) is the bending energy and the second is the shear energy. With independent expansions for  $w$  and  $\theta$ , (1) can be employed to derive beam element stiffness matrices. The case we are interested in is when both  $w$  and  $\theta$  are assumed to behave linearly over an element. This leads to a four-degree-of-freedom element in which displacement and rotation are the nodal degrees-of-freedom. By virtue of the fact  $d\theta/dx$  is constant within this element, the bending energy may be exactly evaluated by one-point Gaussian quadrature. On the other hand, two-point Gaussian quadrature is required to exactly integrate the shear energy term due to the explicit presence of  $\theta$ , which is linear within the element. Employing one-point quadrature on the shear energy term 'underintegrates' the element and it is our prime concern here to ascertain the effect of this procedure. (See also Gallagher<sup>2</sup> pp. 364–367.)

A series of test computations were performed to determine the behaviour of the element. A cantilever beam subjected to an end load (see Figure 1) was analysed for various discretizations. The first example is for a relatively deep beam. The data are:

$$E = 1000 \quad G = 375 \quad t = 1 \quad L = 4$$

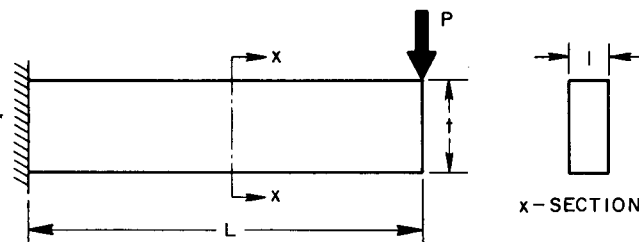


Figure 1. Cantilever beam subjected to end load

Tip displacement results for several discretizations are presented in Table I. As is evident, the one-point quadrature results are vastly superior to the two-point results. A more severe test for linear elements is bending governed by Bernoulli–Euler theory. In this case shear strains are to be equal to zero. Such a situation can be brought about in the present theory if depth is taken very small compared with element length. Alternatively, a very large fictitious value of  $G$  can be specified. In the second example we attempt to ascertain the behaviour of the linear element when the assumptions of the Bernoulli–Euler theory apply. The data of the previous example are employed with the exception of  $G$  which is set here to  $375 \times 10^5$ . Results are listed in Table

Table I. Normalized tip displacement for a deep cantilever beam

Number of elements	Tip displacement— one-point quadrature	Tip displacement— two-point quadrature
1	0.762	$0.416 \times 10^{-1}$
2	0.940	0.445
4	0.985	0.762
8	0.996	0.927
16	0.999	0.981

II. The one-point quadrature results are quite accurate whereas the two-point results are in error by approximately three orders of magnitude. Early attempts at developing bending elements with simple shape functions were abandoned because of results like those for the two-point quadrature presented here.

Table II. Normalized tip displacement for a thin cantilever beam

Number of elements	Tip displacement— one-point quadrature	Tip displacement— two-point quadrature
1	0.750	$0.200 \times 10^{-4}$
2	0.938	$0.800 \times 10^{-4}$
4	0.984	$0.320 \times 10^{-3}$
8	0.996	$0.128 \times 10^{-3}$
16	0.999	$0.512 \times 10^{-3}$

We shall now proceed to give a heuristic argument why two-point quadrature causes such an overly stiff element. Consider a cantilever beam discretized into  $N$  elements. In the assembled stiffness matrix there are  $2N$  degrees-of-freedom—two degrees-of-freedom per element. The shear contribution to the stiffness represents a constraint on the shear strains. If one-point quadrature is employed, one constraint is imposed upon the element, whereas if two-point quadrature is employed, two constraints are imposed upon the element. In the latter case the number of constraints per element equals the number of degrees-of-freedom per element, and the result is that the mesh ‘locks’.

This can be seen more precisely by looking at the stiffness contributions of the bending and shear terms. We assume the nodal degrees-of-freedom are ordered as follows:  $w_1, \theta_1, w_2, \theta_2$ ; and  $h$  is the element length. The stiffnesses are:

$$k_b = \frac{Et^3}{12h} \begin{bmatrix} 0 & 0 & 0 & 0 \\ 0 & 1 & 0 & -1 \\ 0 & 0 & 0 & 0 \\ 0 & -1 & 0 & 1 \end{bmatrix} \quad (2a)$$

$$k_s^{(1)} = \frac{\kappa Gt}{h} \begin{bmatrix} 1 & h/2 & -1 & h/2 \\ h/2 & h^2/4 & -h/2 & h^2/4 \\ -1 & -h/2 & 1 & -h/2 \\ h/2 & h^2/4 & -h/2 & h^2/4 \end{bmatrix} \quad (2b)$$

$$k_s^{(2)} = \frac{\kappa G t}{h} \begin{bmatrix} 1 & h/2 & -1 & h/2 \\ h/2 & h^2/3 & -h/2 & h^2/6 \\ -1 & -h/2 & 1 & -h/2 \\ h/2 & h^2/6 & -h/2 & h^2/3 \end{bmatrix} \quad (2c)$$

where  $k_b$  is the bending stiffness, and  $k_s^{(1)}$  and  $k_s^{(2)}$  are the one-point and two-point quadrature shear stiffnesses, respectively. It is easily verified that the rank of  $k_s^{(1)}$  is one and the rank of  $k_s^{(2)}$  is two. In the latter case,  $k_b$  is completely dominated by the shear stiffness, as the following simple example illustrates.

Consider the case of a one-element cantilever beam, subjected to an end load  $P$  and moment  $M$ .

(i) *One-point quadrature*

Combining (2a) and (2b), eliminating appropriate rows and columns, and solving for the tip displacement and rotation yields

$$w = (h^2/4\alpha + \beta^{-1})P + hM/2\alpha, \quad (3a)$$

$$\theta = (hP/2 + M)/\alpha, \quad (3b)$$

where

$$\alpha = Et^3/12h, \quad (3c)$$

$$\beta = \kappa G t/h. \quad (3d)$$

In the thin beam limit (i.e., when  $\beta \gg \alpha$ ), (3a) becomes

$$w = h(hP/2 + M)/2\alpha, \quad (4)$$

and (3b) remains unchanged. Thus we are left solely with the deformation due to bending as is right.

(ii) *Two-point quadrature*

Carrying out the same steps as in case (i), with (2c) in place of (2b), yields

$$w = \left( \frac{\alpha + h^2\beta/3}{\beta\gamma} \right) P + hM/2\gamma, \quad (5a)$$

$$\theta = (hP/2 + M)/\gamma, \quad (5b)$$

where

$$\gamma = \alpha + h^2\beta/12. \quad (5c)$$

In the thin beam limit (5a) and (5b) become

$$w = (4P + 6M/h)/\beta, \quad (6a)$$

$$\theta = 6(hP + 2M)/h^2\beta, \quad (6b)$$

respectively. In this case only deformations due to shear are in evidence and (6a) and (6b) are  $O(t^{-2})$  in error.

In passing we note that there are some circumstances in which the present element may have some practical value. For example, an axisymmetric shell version might be useful for shell

covered solids in which bilinear elements are used to model the solid. The fact that only one quadrature point is involved may lead to more economical computations in non-linear analysis.

### BILINEAR PLATE BENDING ELEMENT

The strain energy for an isotropic, linear elastic plate, including shear deformation, is

$$U(w, \theta_1, \theta_2) =$$

$$\begin{aligned} & \frac{Et^3}{24(1-\nu^2)} \left\{ \iint_A \left[ \left( \frac{\partial \theta_1}{\partial x_1} \right)^2 + 2\nu \frac{\partial \theta_1}{\partial x_1} \frac{\partial \theta_2}{\partial x_2} + \left( \frac{\partial \theta_2}{\partial x_2} \right)^2 + \frac{(1-\nu)}{2} \left( \frac{\partial \theta_1}{\partial x_2} + \frac{\partial \theta_2}{\partial x_1} \right)^2 \right] dx_1 dx_2 \right. \\ & \left. + \frac{6\kappa(1-\nu)}{t^2} \iint_A \left[ \left( \frac{\partial w}{\partial x_1} - \theta_1 \right)^2 + \left( \frac{\partial w}{\partial x_2} - \theta_2 \right)^2 \right] dx_1 dx_2 \right\}, \end{aligned} \quad (7)$$

where  $x_1$  and  $x_2$  are cartesian co-ordinates,  $w$  is the transverse displacement,  $\theta_1$  and  $\theta_2$  are the rotations about the  $x_1$  and  $x_2$  axes, respectively,  $E$  is Young's modulus,  $\nu$  is Poisson's ratio,  $\kappa$  is the shear correction factor,  $t$  is the plate thickness and  $A$  is its area. The first integral in (7) represents the bending energy and the second represents the shear energy. We consider a four-node quadrilateral element and assume the displacement and rotations are expanded in independent bilinear shape functions. The isoparametric concept is employed.<sup>1</sup> This results in three degrees-of-freedom—one displacement and two rotations—at each of the corners.

For very thick plates two-by-two Gaussian quadrature leads to acceptable results, however, for thin plates it causes 'locking' as indicated for the beam in the previous section. In this case we use two-by-two Gaussian quadrature on the bending energy term and one-point Gaussian quadrature on the shear energy term. This results in one constraint per element. In large meshes there are approximately three equations per element, thus there is no danger of the mesh 'locking'. As is apparent, the proposed element is extremely simple, and easily and concisely coded. We are certain that the element routines are faster than any other plate bending element yet proposed. In the next section we will show that the element is also surprisingly accurate.

### NUMERICAL EXAMPLES: THIN PLATES

In this section we present several numerical examples which have become more or less standard ones for evaluating plate elements. All computations were performed on a CDC 6400 computer in single precision. (A single precision word consists of 60 bits on the CDC 6400.)

#### *Square plate*

The data for this example consists of the following (see Figure 2):

$$E = 10.92 \times 10^5 \quad \nu = 0.3 \quad t = 0.1 \quad L = 10$$

Both simply supported and clamped boundary conditions were considered as well as concentrated and uniformly distributed loadings. Results are presented in Tables III and IV for  $\kappa$  values of 1000 and 5/6. The former value is set to artificially maintain the Poisson–Kirchhoff constraint. Due to the fact that the plate is rather thin ( $L/t = 100$ ), there is little difference in the results for the two values of  $\kappa$ . In fact, the bending moments are identical. In practical situations there seems no point in exceeding the 'natural' value of  $\kappa = 5/6$ .

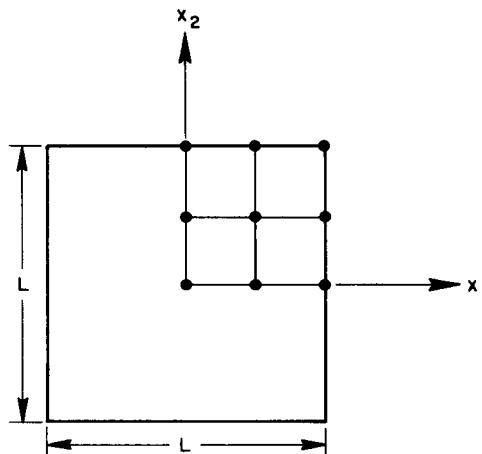


Figure 2. Square plate. Due to symmetry only one quadrant is discretized

Table III. Normalized centre displacement and bending moment for a simply supported square plate

Number of elements	Displacement—concentrated load	Displacement—uniform load	Moment—uniform load
4	0.9922	0.9770	0.851
16	0.9948	0.9947	0.963
64	0.9982	0.9987	0.991
(a) $\kappa = 1000$			
Number of elements	Displacement—concentrated load	Displacement—uniform load	Moment—uniform load
4	0.9957	0.9782	0.851
16	0.9991	0.9960	0.963
64	1.0034	0.9997	0.991
(b) $\kappa = \frac{5}{6}$			

Moment and shear resultants, and displacements are plotted in Figure 3 along the line  $x_1 = 0$ , for the clamped, concentrated load case in which  $\kappa = 5/6$ . Along  $x_1 = 0$  and  $x_2 = 0$ , the  $x_1$  and  $x_2$  components of the moment are equal, as are the  $x_1$  and  $x_2$  components of the shear.

The simply supported concentrated load case has, it seems, taken on the role of the pre-eminent comparison problem for bending elements. In Figure 4 the present element, with  $\kappa = 1000$ , is compared with data taken from Gallagher.<sup>2</sup> The good convergence of the element is evident.

#### Clamped circular plate

The data for this example is the same as for the previous problem except (see Figure 5):

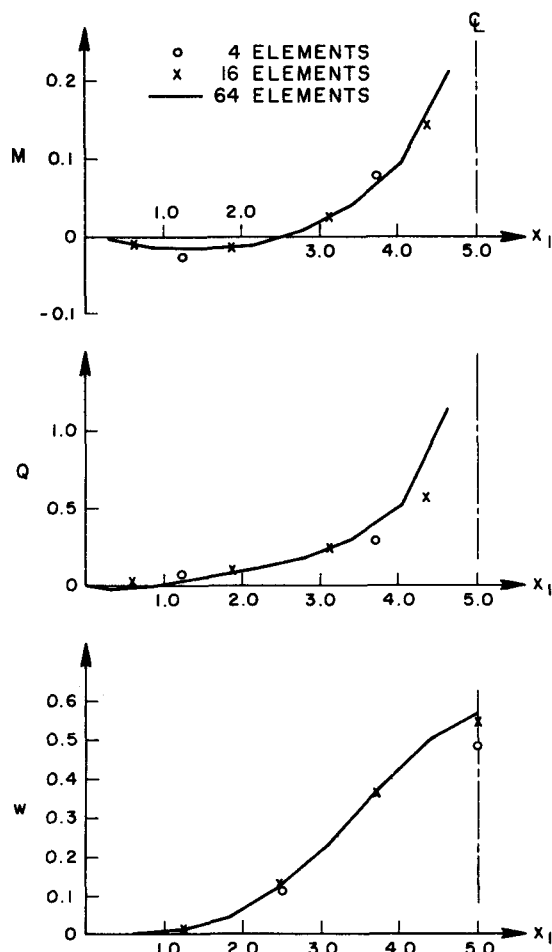
$$R = 5 \quad t = 0.1$$

Table IV. Normalized centre displacement and bending moment for a clamped square plate

Number of elements	Displacement—concentrated load	Displacement—uniform load	Moment—uniform load
4	0.8652	0.9535	0.822
16	0.9650	0.9850	0.955
64	0.9920	0.9937	0.986

(a)  $\kappa = 1000$

Number of elements	Displacement—concentrated load	Displacement—uniform load	Moment—uniform load
4	0.8720	0.9575	0.822
16	0.9748	0.9890	0.955
64	1.0034	0.9976	0.986

(b)  $\kappa = \frac{5}{6}$ Figure 3. Moment ( $M$ ), shear resultant ( $Q$ ) and displacement ( $w$ ) versus edge co-ordinate ( $x_1$ ) for a clamped square plate subjected to a concentrated load



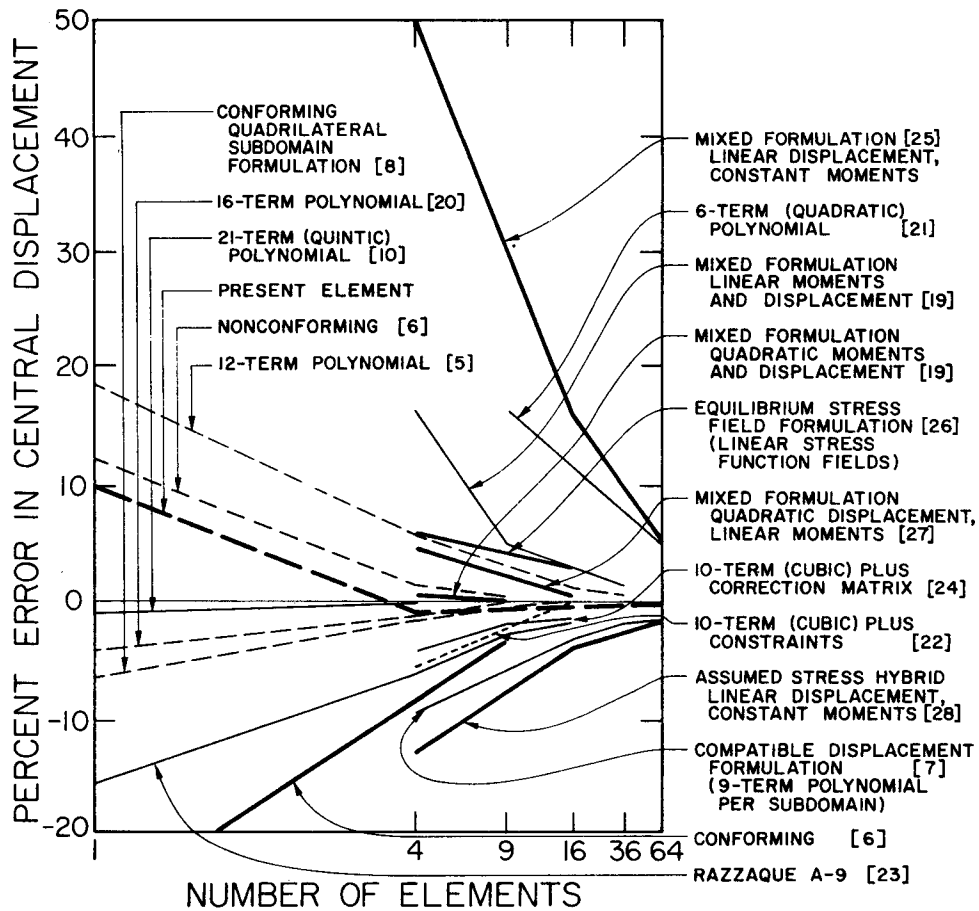


Figure 4. Simply supported square plate subjected to a concentrated load. Comparison of centre displacement for various bending elements

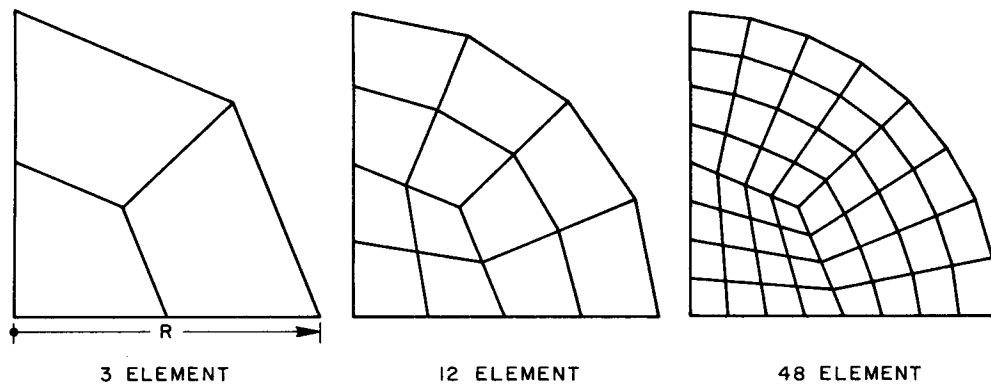


Figure 5. Finite element meshes for clamped circular plate. Due to symmetry only one quadrant is discretized

Results are presented in Table V for concentrated and uniform loadings, and  $\kappa$  values of 1000 and 5/6.

Again, due to the thinness of the plate, there is little difference in the displacement results for the two values of  $\kappa$ , and the moment results are identical.

Table V. Normalized centre displacement and bending moment for a clamped circular plate

Number of elements	Displacement—concentrated load	Displacement—uniform load	Moment—uniform load
3	0.9197	0.8587	0.827
12	0.9579	0.9535	0.957
48	0.9883	0.9888	0.990
(a) $\kappa = 1000$			
Number of elements	Displacement—concentrated load	Displacement—uniform load	Moment—uniform load
3	0.9267	0.8621	0.827
12	0.9674	0.9570	0.957
48	1.0005	0.9925	0.990
(b) $\kappa = \frac{5}{6}$			

### NUMERICAL SENSITIVITY DUE TO EXTREME THINNESS

The results of the previous section indicate that despite the simplicity of the present element it is quite accurate. However, precaution must be taken when employing elements derived from the reduced integration concept. This admonition stems from the observation that the shear stiffness is  $O((h/t)^2)$  times the bending stiffness. (In the case of a quadrilateral bending element  $h$  may be taken to be the length of the longest side.) For fixed  $h$ , as  $t \rightarrow 0$ , it is only a matter of time before the effect of the bending stiffness vanishes completely due to the finite computer word length. Results of this kind can be seen for the beam element in Figure 6 and for the plate element in Figure 7. The plateaus represent the appropriate solutions for the meshes in question in the 'thin' limit. Deterioration of the numerical solution begins to occur at  $L/t = 10^4$  in the case of the beam, and  $L/t = 10^5$  for the plate; this corresponds to element aspect ratios (i.e.,  $h/t$ ) of  $10^4/16$  and  $10^5/8$ , respectively. It is unlikely that aspect ratios larger than these values will be met in practice. However, on computers with shorter single precision word length, deterioration will commence at smaller aspect ratios. Here it is important to employ a strategy which circumvents these difficulties. This can be done as follows: Determine the maximum element aspect ratio for which good results are obtained by plotting graphs similar to Figures 6 and 7. Before combining the shear and bending contributions of the element stiffness, test the aspect ratio. If it is less than the value for which good results are obtained, combine in the usual way. Otherwise, multiply the shear stiffness by  $(t/h)^2$  times the square of the maximum element aspect ratio allowed, then combine. This will reduce the disparity between the bending and shear term to an acceptable level, yet maintain thin element behaviour. Numerical results illustrating these ideas are depicted in Figures 6 and 7. The maximum allowable aspect ratios were determined to be  $10^4/16$  for the beam element and  $10^5/8$  for the plate element, from Figures 6 and 7,

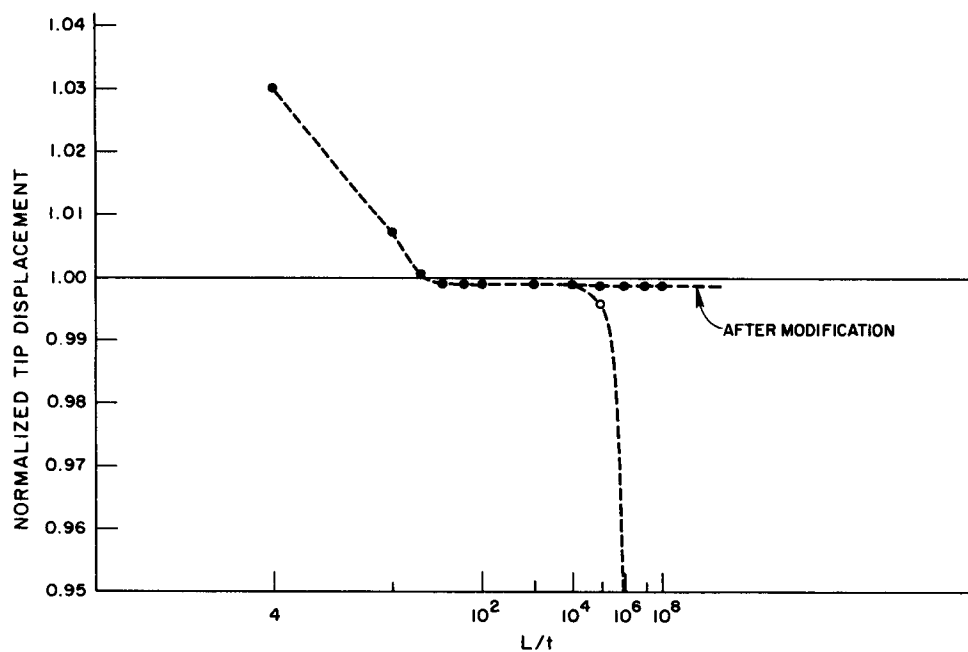


Figure 6. 16 element cantilever beam subjected to tip load. Normalized tip displacement *versus* aspect ratio

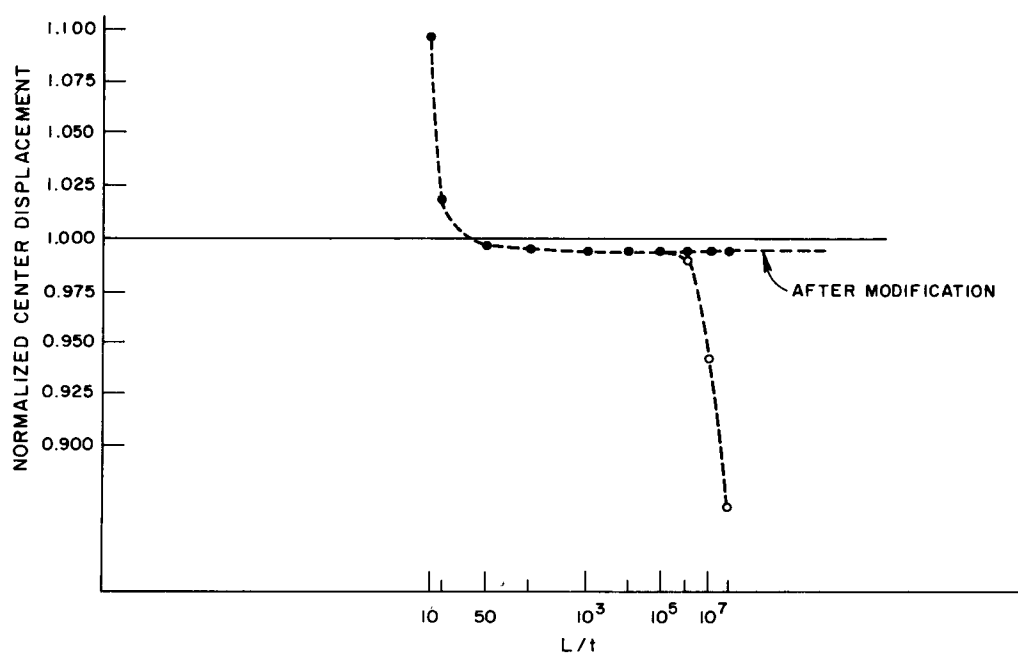


Figure 7. 16 element model of simply supported square plate subjected to uniform load. Normalized centre displacement *versus* aspect ratio

respectively. Employing these values in the procedure described above enables the plateaus to be extended to the higher aspect ratios, as illustrated in Figures 6 and 7. This process enables the reduced integration procedure to be applied successfully in cases involving arbitrarily large aspect ratios.

Of course, another way to avoid difficulties is to work in double precision on short word computers.

### APPLICATION TO THICK PLATES

One-point Gaussian quadrature on the shear term has a decidedly beneficial effect in application to thin plates. However, the opposite is true for very thick plates. The difficulties do not always manifest themselves. For example, results for the uniformly loaded clamped circular plate are acceptable (See Figure 8;  $q$  refers to the magnitude of the load). For  $t/R = 0.4$  the results are of about the same level of accuracy as those in Reference 18, where a higher-order element is employed. On the other hand, results for the same plate subjected to a concentrated load tend to oscillate about the exact solution (see Figure 9). This problem is a trying one as the exact Reissner's theory solution consists of an infinite displacement under the load, viz.

$$w = \frac{PR^2}{16\pi D} \left[ \underbrace{\left(1 - \frac{r^2}{R^2}\right) - \frac{2r^2}{R^2} \ln \frac{R}{r}}_{\text{bending}} - \underbrace{\frac{8D}{\kappa G t R^2} \ln \frac{r}{R}}_{\text{shear}} \right]$$

$$\beta = \frac{PR}{4\pi D} \left[ \frac{r}{R} \ln \frac{R}{r} \right]$$

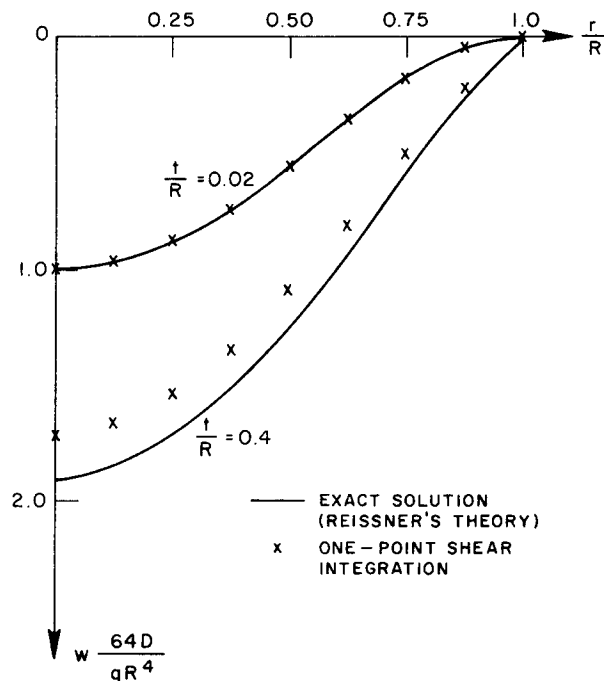


Figure 8. Clamped circular plate subjected to uniform load (48 element model). Comparison of underintegrated shear element with exact solution

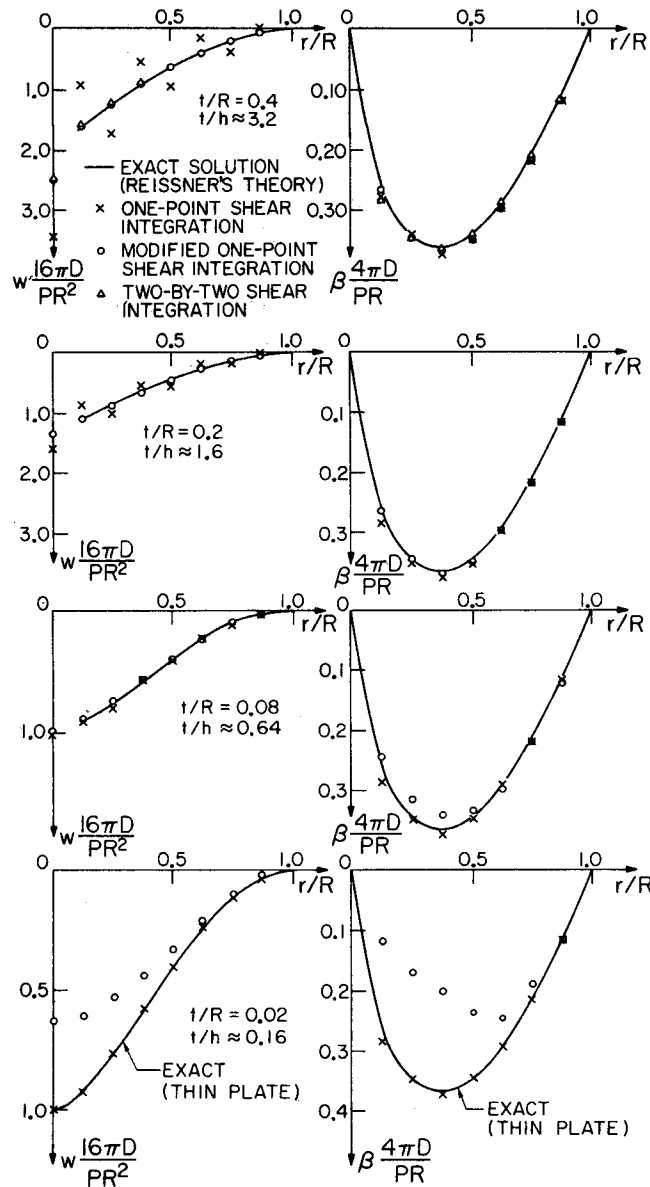


Figure 9. Clamped circular plate subjected to concentrated load (48 element model). Comparison of underintegrated shear elements with exact solution

where  $P$  is the concentrated force and  $D$  is the bending rigidity. As the plate thickness is reduced the oscillations are lessened. From these results we conclude that **when the  $t/h$  ratio exceeds unity, the one-point Gaussian quadrature of the shear term should be abandoned in favour of the following scheme: Two-by-two Gaussian quadrature should be used on the  $(\partial w/\partial x_1)^2$  and  $(\partial w/\partial x_2)^2$  contributions to the shear energy. The remaining terms in the shear energy should be integrated as usual by one-point Gaussian quadrature. We refer to this element as the 'modified' one-point shear element.**

However, we note that even in the unmodified case the stresses are very good and the values of the displacements at the element midsides (equivalently the node-to-node averages) are also very good.

A spectral analysis of the element stiffness, when one-point Gaussian quadrature is employed on the shear term, reveals that there are five zero eigenvalues—two more than the usual three rigid body modes. Thus the element by itself is rank deficient, but this only manifests itself in problems for very thick plates and here only in certain cases. The two additional zero-energy modes are illustrated in Figure 10. The first mode consists of  $\theta_1 = \theta_2 = 0$  and an ‘hourglass’ pattern for  $w$ .<sup>29</sup> Modifying the one-point shear integration as indicated above removes the hourglass mode and leads to good results for very thick plates as evidenced by Figure 9. The second mode consists of  $w = 0$  and an in-plane twisting of the plate. In a mesh in which the rigid body modes are removed, this pattern cannot persist and thus causes no further rank deficiency.

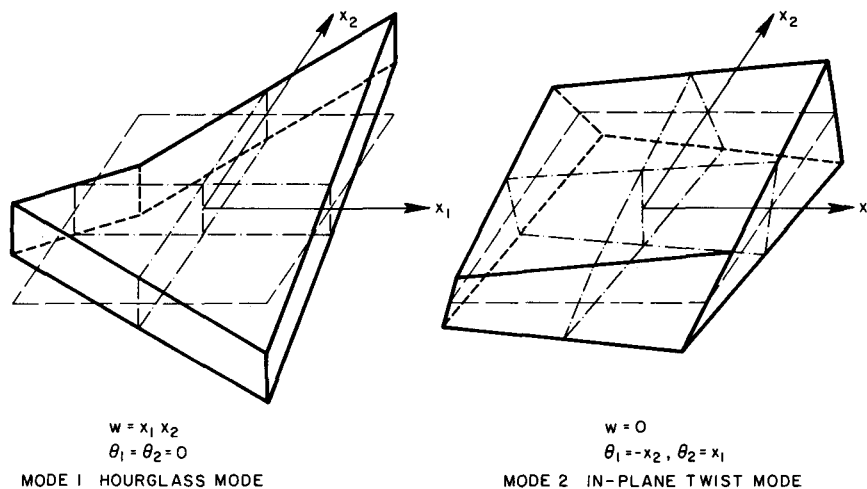


Figure 10. Zero-energy modes of underintegrated plate bending element

## CONCLUSIONS

We have presented an element for the bending of thin and moderately thick plates which involves minimal programming, is highly efficient and competitively accurate. Due to these attributes the element offers an attractive basis for non-linear developments. Numerical sensitivity in applications involving extremely thin elements has been shown to be avoidable by employing a simple computational strategy. Very thick plates may be successfully analyzed by a slight modification to the element.

## ACKNOWLEDGEMENT

The authors would like to thank T. Shugar of the Civil Engineering Laboratory, Port Hueneme, California, L. Ovenshire of the National Highway Traffic Safety Administration of the Department of Transportation and K. Saczalski of the Office of Naval Research, for continued support and interest.

## REFERENCES

1. O. C. Zienkiewicz, *The Finite Element Method in Engineering Science*, McGraw-Hill, New York, 1971.
2. R. H. Gallagher, *Finite Element Analysis Fundamentals*, Prentice-Hall, Englewood Cliffs, N.J., 1975.
3. R. D. Cook, *Concepts and Applications of Finite Element Analysis*, Wiley, New York, 1974.
4. B. M. Irons and K. J. Draper, 'Inadequacy of nodal connections in a stiffness solution for plate bending', *AIAA J.*, **4**, 961 (1965).
5. R. J. Melosh, 'Basis for derivation of matrices for the direct stiffness method', *AIAA J.*, **1**, 1631–1637 (1963).
6. G. P. Bazely, Y. K. Cheung, B. M. Irons and O. C. Zienkiewicz, 'Triangular elements in plate bending—conforming and non-conforming solutions', *Proc. Conf. Matrix Meth. Struct. Mech.*, Wright-Patterson A.F.B., Ohio, 547–576 (1965).
7. R. W. Clough and J. L. Tocher, 'Finite element stiffness matrices for analysis of plate bending', *Proc. Conf. Matrix Meth. Struct. Mech.*, Wright-Patterson A.F.B., Ohio, 515–545 (1965).
8. B. Fraeijs de Veubeke, 'A conforming finite element for plate bending', *Int. J. Solids and Struct.*, **4**, 95–108 (1968).
9. K. Bell, 'A refined triangular plate bending finite element', *Int. J. num. Meth. Eng.*, **1**, 101–122 (1969).
10. G. R. Cowper, E. Kosko, G. Lindberg and M. Olson, 'Static and dynamic applications of a high precision triangular plate bending element', *AIAA J.*, **7**, 1957–1965 (1969).
11. G. Butlin and R. Ford, 'A compatible triangular plate bending finite element', *Int. J. Solids and Struct.*, **6**, 323–332 (1970).
12. T. H. H. Pian, 'Element stiffness matrices for boundary compatibility and for prescribed boundary stresses', *Proc. Conf. Matrix Meth. Struct. Mech.*, Wright-Patterson A.F.B., Ohio, 457–478 (1965).
13. G. Wempner, J. T. Oden and D. Kross, 'Finite element analysis of thin shells', *Proc. ASCE, J. Eng. Mech. Div.*, **94**, 1273–1294 (1968).
14. J. A. Stricklin, W. E. Haisler, P. R. Tisdale and R. Gunderson, 'A rapidly converging triangular plate bending element', *AIAA J.*, **7**, 180–181 (1969).
15. I. Fried, 'Shear in  $C^0$  and  $C^1$  plate bending elements', *Int. J. Solids and Struct.*, **9**, 449–460 (1973).
16. I. Fried, 'Residual energy balancing technique in the generation of plate bending finite elements', *Computers and Structures*, 771–778 (1974).
17. I. Fried and S. K. Yang, 'Triangular, nine-degree-of-freedom,  $C^0$  plate bending element of quadratic accuracy', *Quart. Appl. Math.*, **31**, 303–312 (1973).
18. O. C. Zienkiewicz, R. L. Taylor and J. M. Too, 'Reduced integration technique in general analysis of plates and shells', *Int. J. num. Meth. Eng.*, **3**, 575–586 (1971).
19. J. Bron and G. Dhatt, 'Mixed quadrilateral elements for bending', *AIAA J.*, **10**, 1359–1361 (1972).
20. F. K. Bogner, R. L. Fox and L. A. Schmit, 'The generation of interelement, compatible stiffness and mass matrices by the use of interpolation formulas', *Proc. 1st. Conf. Matrix Meth. Struct. Mech.*, Wright-Patterson A.F.B., Ohio, 397–443 (1965).
21. L. S. D. Morley, 'The constant-moment plate bending element', *J. Strain Analysis*, **6**, 20–24 (1971).
22. J. W. Harvey and S. Kelsey, 'Triangular plate bending elements with enforced compatibility', *AIAA J.*, **9**, 1023–1026 (1971).
23. A. Q. Razzaque, 'Program for triangular elements with derivative smoothing', *Int. J. num. Meth. Engng.*, **6**, 333–344 (1973).
24. F. Kikuchi and Y. Ando, 'Some finite element solutions for plate bending problems by simplified hybrid displacement method', *Nuc. Eng. Design*, **23**, 155–178 (1972).
25. L. R. Herrmann, 'Finite element bending analysis of plates', *J. Eng. Mech. Div.*, **94**, 13–25 (1968).
26. Z. M. Elias, 'Duality in finite element methods', *J. Eng. Mech. Div.*, **94**, 931–946 (1968).
27. W. Visser, 'A refined mixed-type plate bending element', *AIAA J.*, **7**, 1801–1802 (1969).
28. R. D. Cook, 'Some elements for analysis of plate bending', *J. Eng. Mech. Div.*, **98**, 1452–1470 (1972).
29. S. W. Key, 'A finite element procedure for the large deformation dynamic response of axisymmetric solids', *Computer Meth. in Appl. Mech. and Engng.*, **4**, 195–218 (1974).